Solid State Communications 231-232 (2016) 17–25

Contents lists available at ScienceDirect

Solid State Communications

journal homepage: www.elsevier.com/locate/ssc

Pressure-induced phase transitions and structural properties of CoF_2: An ab-initio molecular dynamics study

Cihan Kürkçü [a,*], Ziya Merdan [b], Hülya Öztürk [a]

[a] Department of Physics, Ahi Evran University, Kirsehir, Turkey
[b] Department of Physics, Gazi University, Ankara, Turkey

ARTICLE INFO

Article history:
Received 27 July 2015
Received in revised form
7 January 2016
Accepted 15 January 2016
Available online 2 February 2016

Keywords:
Cobalt fluoride
Ab initio
Phase transitions
Molecular dynamics

ABSTRACT

The crystal structure of CoF_2 was studied theoretically using first-principles density functional theory (DFT) methods within the generalized gradient approximation (GGA) and local density approximation (LDA) under rapid hydrostatic pressure up to 144 GPa. CoF_2 undergoes a structural phase transformation from the rutile-type tetragonal parent phase with space group $P4_2/mnm$ to the $CaCl_2$-type orthorhombic parent phase with space group Pnnm at 64 GPa with GGA and at 96 GPa with LDA methods. Another phase transformation occurs from the $CaCl_2$-type structure to monoclinic parent phase with space group $P2_1/c$ at 96 GPa with a GGA method. These phase transitions are also studied by enthalpy and total energy calculations. According to these calculations, we obtained the first phase transformation at about 6.5 GPa both GGA and LDA methods and the later phase transformation at about 45 GPa with the GGA method.

1. Introduction

Because of the novel phase transitions and geophysical importance, the difluoride compounds have been studied under the influence of pressure and temperature [1–9]. Cobalt (II) Fluoride is a pink crystalline solid compound which is antiferromagnetic at low temperature. It can be used as a catalyst to alloy metals and for optical deposition.

CoF_2 crystallizes in a tetragonal rutile-type structure (D_{4h}^{14}, $P4_2/mnm$, $Z=2$) under ambient conditions. Its unit cell consists of two cobalt and four fluorine atoms. The cobalt (Co) atoms are located at $(0,0,0),(\frac{1}{2},\frac{1}{2},\frac{1}{2})$, and fluorine atoms at $(x,x,0),(-x,-x,0)$, $(\frac{1}{2}+x,\frac{1}{2}-x,\frac{1}{2})$ and $(\frac{1}{2}-x,\frac{1}{2}+x,\frac{1}{2})$, where x has a value about 0.3 and is the only internal coordinate that is not fixed by symmetry [8].

A number of investigations associated with phase transitions of rutile-structured difluorides NiF_2, MgF_2, FeF_2 and ZnF_2 etc. have been studied [9–13]. Compounds with this rutile-type structures have received considerable attention in solid state geophysics because of their crystal structure analogy with stishovite (high-pressure form of SiO_2) considered to be one of the important phase in various proposed models of the Earth's deep interior.

Phase transitions in this compound have been studied in 1969, by Austin [1], up to 9 GPa. He observed an orthorhombic phase. Later, Nagel and O'Keeffe [7] suggested that this phase is $CaCl_2$-type structure, a slight distortion of rutile structure. Kabalkina et al. [14] reported that rutile-type of CoF_2 transforms into the "distorted fluorite" phase at about 10 GPa. Ming et al. [6] investigated structure of CoF_2 up to 37 GPa. They observed a phase transition from rutile-type tetragonal structure to "distorted fluoride" phase at about 6.5 GPa, lower than that of Kabalkina's result.

Structural phase transitions can take place in a crystal constitute a fascinating subject in solid state physics. Many experimental studies have been performed on a variety of crystalline systems, while theoretical studies are imposed on structural changes in crystals. The detailed structural properties of the transformation or the transformation mechanism are still not identified due to problems in mapping out the atomistic motions through the experiments. In this study, we propose a simulation study of the transformation mechanism of CoF_2.

2. Computational details

The structural properties of the tetragonal CoF_2 compound are investigated in the generalized gradient approximation and the local density approximation of density functional theory with the functionals of Perdew–Burke–Ernzerhof (PBE) for GGA method [15] and Ceperley and Alder (CA) [16] for LDA method using the

* Corresponding author. Tel.: +90 386 2804644; fax: +90 386 2804525.
E-mail addresses: ckurkcu@ahievran.edu.tr, cihankurkcu@gmail.com (C. Kürkçü).

http://dx.doi.org/10.1016/j.ssc.2016.01.010
0038-1098/

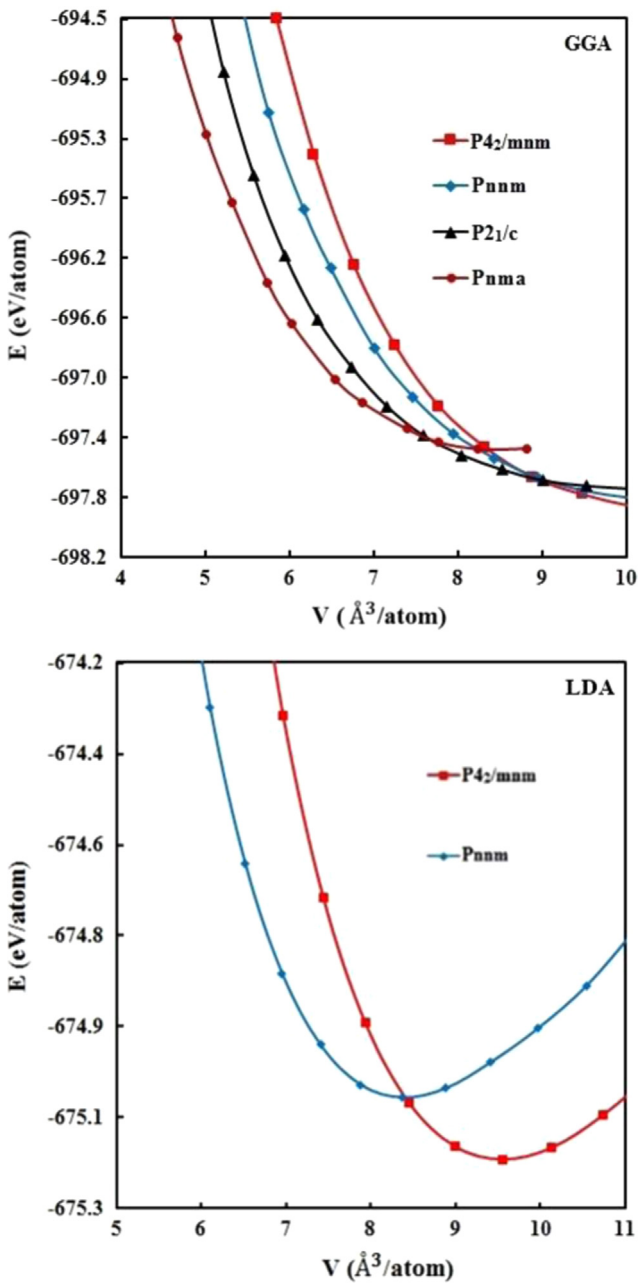

Fig. 1. (Color on-line) Energy–volume curves of CoF_2: $P4_2/mnm$, Pnnm, $P2_1/c$ and Pnma phases with GGA and $P4_2/mnm$ and Pnnm phases with LDA methods.

ab-initio program SIESTA [17]. The self-consistent "norm-conserving" pseudopotentials are generated using the Troullier–Martins scheme [18].

In the LDA approximation, the valance atomic configuration used for Co and F are $3d^74s^2$ and $2s^22p^5$, respectively. This approximation takes only valance electrons of atoms during the calculations because these electrons are playing a considerable role in the physical properties of crystals.

Double-zeta plus polarized orbitals were used in the calculations along with the 150 Ryd mesh cut-off for a real space grid. For the Brillouin Zone (BZ) integration, we use the Monkhorst–Pack (MP) [19] mesh $6 \times 6 \times 6$ for tetragonal $P4_2/mnm$, orthorhombic Pnnm and monoclinic $P2_1/c$ phases. The simulation cell consist of 96 atoms with periodic boundary conditions. We employ $\Gamma-$point sampling for the BZ integration which is plausible for a simulation cell with 96-atoms. These structures were allowed to relax and to find their equilibrium volumes and lowest energies for each value of the applied pressure by optimizing their lattice vectors and atomic positions together until the maximum atomic forces were getting smaller until 0.01 eV $Å^{-1}$ and the stress tolerances were getting less until 0.5 GPa.

CoF_2 crystallizes in a tetragonal rutile-type structure with space group $P4_2/mnm$. CoF_2 shows five different solid structures at high pressures and temperatures. Rutile structure of CoF_2 sequentially transforms orthorhombic $CaCl_2$ structure with space group Pnnm → another orthorhombic distorted PdF_2 structure with space group Pbca or cubic PdF_2 structure with space group $Pa\bar{3}$ in coexistence → another cubic structure with space group $Fm\bar{3}m$ → orthorhombic cotunnite structure with space group Pnma with the influence of high pressure and temperature factors [25].

For this material, the results of our GGA calculations yield the following sequence of the stable phases: $P4_2/mnm \rightarrow Pnnm \rightarrow P2_1/c$. First two phases of CoF_2 are in good agreement with the results of Barreda et al. [25] both GGA and LDA. However, the last phase of CoF_2 for GGA is not in agreement with the results of Barreda et al. [25]. The origin of the disagreement is not clear but we suspect that it is related to kinetic. Our simulations were performed at 0 K while experiments were performed at room or high temperatures.

Pressure was applied via the methods of ParrinelloRahman for GGA and conjugate gradient (CG) for LDA to the system and increased with an increment of 8 GPa for GGA and 6 GPa for LDA. In order to analyze each molecular dynamics (MD) time step for GGA and minimization step for LDA, we use the KPLOT program and RGS algorithm [20–21] that give elaborated knowledge about cell parameters, atomic positions and space group of an analyzed structure.

Table 1
Theoretical ($T=0$ K) CoF_2 lattice parameters for rutile-type structure (space group, SG:$P4_2/mnm$) and high-pressure phases: $CaCl_2$-type structure (SG:Pnnm) both GGA and LDA and monoclinic structure (SG:$P2_1/c$) with GGA at the corresponding pressure *P*. *a*, *b*, and *c* are the lattice parameters, *V* is the equilibrium volume at the respective pressure, B_0 the bulk modulus, $B_0^{'}$ the first derivative of the bulk modulus.

Phases	*P* (GPa)	*a* (Å)	*b* (Å)	*c* (Å)	*V* ($Å^3$)	B_0 (GPa)	$B_0^{'}$	Reference
$P4_2/mnm$ (GGA)	0	4.6611	4.6611	3.1472	68.37	100	3.99	This Study
$P4_2/mnm$(LDA)	0	4.5867	4.5867	3.1316	57.18	101	4.00	This Study
		4.6950	4.6950	3.1780	70.10	104	4.00	[25] (Expt.)
		4.6400	4.6400	4.8000	70.30			[1] (Expt.)
		4.7250	4.7250	3.2220				[3] (Theory)
		4.8110	4.8110	3.2560	75.35			[9] (Theory)
		4.6950	4.6950	3.1817	70.10			[24] (Expt.)
		4.7637	4.7637	3.2013	72.65	97.54	4.49	[25] (Theory)
Pnnm (GGA)	6.5	3.3885	4.8858	3.0546	50.57	120	4.16	This Study
Pnnm (LDA)	6.5	4.8914	4.6820	3.0324	49.14	116	4.10	This Study
		4.6790	4.4850	3.1330	65.70			[25] (Expt.)
		4.7153	4.5275	3.1477	67.20			[25] (Theory)
	6.5							[3] Theory
$P2_1/c$ (GGA)	45	3.5463	2.4117	5.4428	42.90	146	4.37	This Study

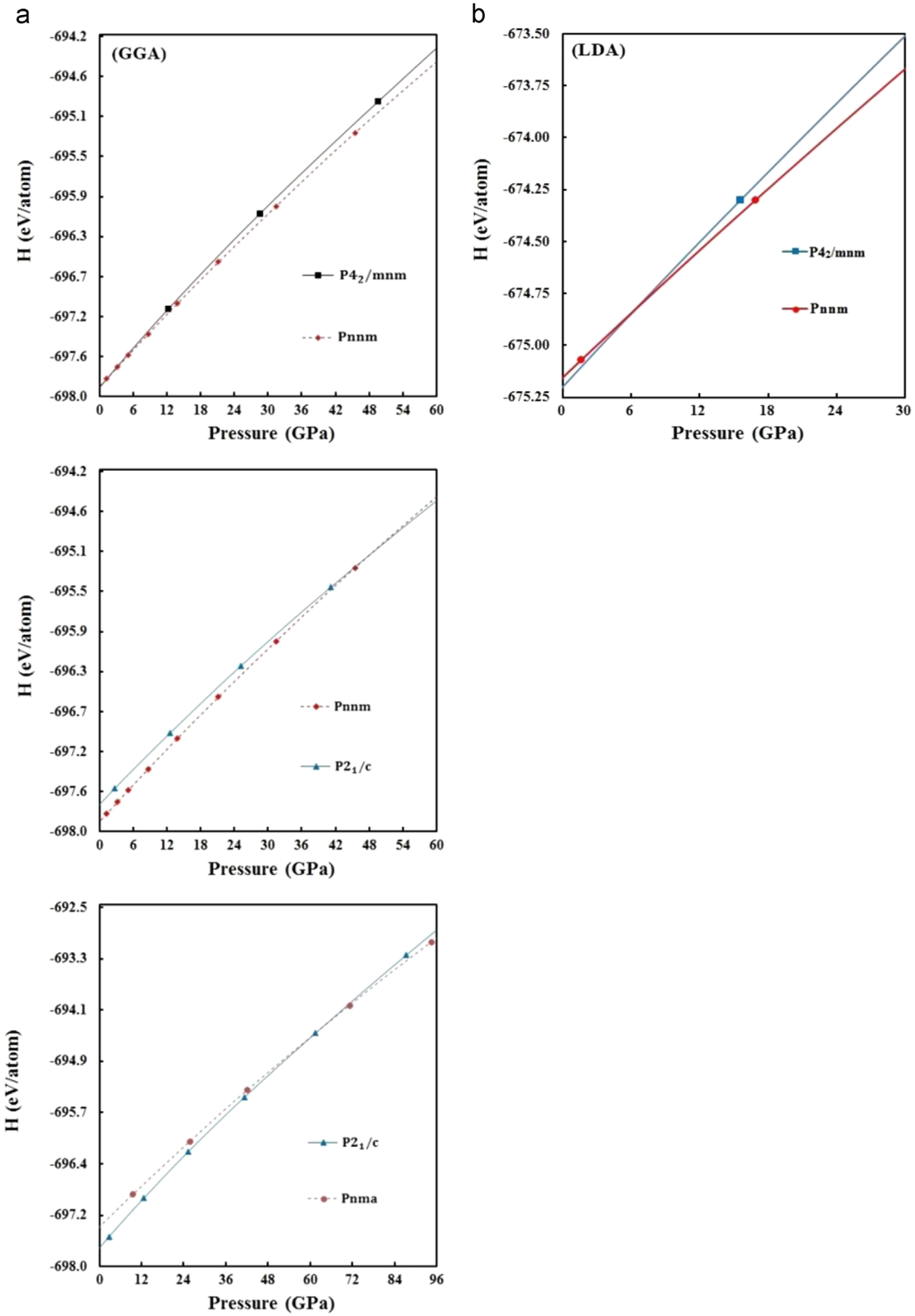

Fig. 2. (Color on-line) Enthalpy curves as a function of pressure for $P4_2/mnm$, Pnnm, $P2_1/c$ and Pnma phases with GGA and $P4_2/mnm$ and Pnnm phases with LDA methods.

3. Results and discussion

The difluorides of the first-row transition metals with tetragonal structure can be produced by a continuous distortion either orthorhombic or monoclinic structure. The experiments revealed phase transitions of CoF_2 under pressure, from the tetragonal rutile-type structure to orthorhombic $CaCl_2$-type structure both GGA and LDA [1,25]. The pressure dependence of the phase transition of CoF_2 was investigated [1,3,6,9,24,25]. Our study showed that the tetragonal structure of CoF_2 transforms to orthorhombic structure and this orthorhombic structure transforms monoclinic structure with GGA. The tetragonal structure transforms to

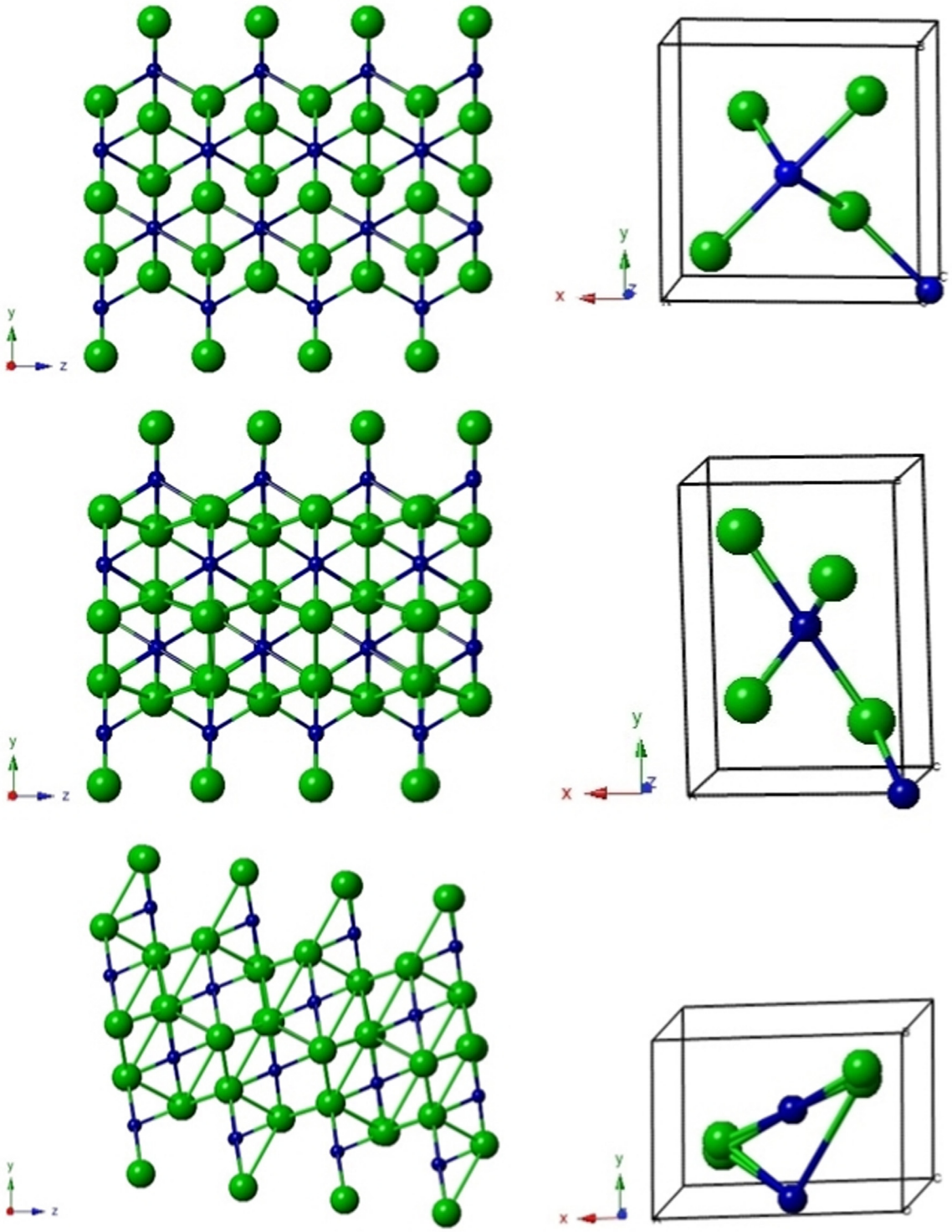

Fig. 3. (Color on-line) Crystal structures with unitcell views of CoF_2: $P4_2/mnm$ phase at zero pressure (top), Pnnm phase at 64 GPa (middle) and $P2_1/c$ phase at 96 GPa (bottom) with the GGA method.

orthorhombic structure with LDA. We first calculated the total energy E_{tot} of tetragonal rutile-type structure with space group $P4_2/mnm$, orthorhombic $CaCl_2$-type structure with space group Pnnm, monoclinic structure with space group $P2_1/c$ and another orthorhombic cotunnite structure with space group Pnma of CoF_2 illustrated in Fig. 1 for GGA and LDA. Although we have not obtained Pnma phase of CoF_2 both LDA and GGA calculations, we studied the energy–volume and pressure–enthalpy relation of the known Pnma phase of CoF_2 to compare the energetic of the phases predicted in this study with them. After that, we make a fit of these energy–volume data to the third-order Birch–Murnaghan equation of state given by:

$$P = 1.5\,B_0\left[(V/V_0)^{-\frac{7}{3}} - (V/V_0)^{-\frac{5}{3}}\right] x\left\{1+0.75\,(B_0^{'}-4)\left[(V/V_0)^{-\frac{2}{3}}-1\right]\right\} \quad (1)$$

where P is the applied pressure, V is the volume at pressure, V_0, B_0 and $B_0^{'}$ are the volume, bulk modulus and its pressure derivative at

Table 2
The equilibrium lattice parameters and the atomic fractional coordinates of the $P4_2/mnm$, Pnnm and $P2_1/c$ phases.

Phases	a (Å)	b (Å)	c (Å)	x	y	z
$P4_2/mnm$ (GGA)	4.6611	4.6611	3.1472	Co: 0.0000	0.0000	0.5000
$P4_2/mnm$ (LDA)	4.5867	4.5867	3.1316	F: 0.1947	0.8053	0.0000
				F: 0.8053	0.1947	0.0000
Pnnm (GGA)	3.3885	4.8858	3.0546	Co: 0.0000	0.0000	0.0000
Pnnm (LDA)	4.8914	4.6820	3.0324	F: 0.7086	0.3065	0.0000
				F: 0.2914	0.6935	0.0000
$P2_1/c$ (GGA)	3.5463	2.4117	5.4428	Co: 0.5000	0.0000	0.5000
				F: 0.1797	0.7231	0.1752
				F: 0.8203	0.2231	0.3248

ambient pressure, respectively [22,23]. The lattice parameters a, b, c, volume V, bulk modulus B_0 and its first derivative $B_0^{'}$ obtained from our study for $P4_2/mnm$, Pnnm and $P2_1/c$ phases with GGA and $P4_2/mnm$, Pnnm phases with LDA methods are given in Table 1, together with other theoretical and experimental results.

We used the Gibbs free energy in order to decide the most thermodynamic stable phase at a given pressure and temperature. The most stable phase of CoF_2 is $P4_2/mnm$. The Gibbs free energy is described as below:

$$G = E_{tot} + PV - TS \tag{2}$$

where E, P, V and S are the total energy, pressure, volume and entropy, respectively. Our theoretical calculations are achieved at 0 K, therefore, the TS term is neglected. Thus, Gibbs free energy G equals to the enthalpy as follows:

$$H = E_{tot} + PV \tag{3}$$

where $P = -\partial E_{tot}/\partial V$. As structural phase transitions in the simulations take place across the whole simulation cells, the systems have to cross a noteworthy energy barrier to change from one phase to another one. Therefore the simulated structures should be overpressurized so as to obtain a phase transition. Enthalpy calculations give often reasonable transition pressures relative to experiments. The intersection of two enthalpy curves shows a pressure-induced phase transition between two phases. To determine the transition pressures, enthalpy curves were plotted as a function of pressure for $P4_2/mnm$, Pnnm, $P2_1/c$ and Pnma phases for GGA in Fig. 2a and $P4_2/mnm$ and Pnnm phases for LDA in Fig. 2b. We use the energy–volume data for enthalpy calculations. The phase transitions from tetragonal $P4_2/mnm$ to orthorhombic Pnnm phase, from Pnnm to monoclinic $P2_1/c$ phase and from $P2_1/c$ to orthorhombic Pnma phase were predicted at pressures of about 6.5 GPa both GGA and LDA methods and about 45 GPa and 56 GPa with a GGA method in CoF_2, respectively.

By using the GGA method, it was found that Co is six-, six- and four-fold coordinated by F for the rutile-type structure, $CaCl_2$-type structure and $P2_1/c$ phase, respectively. The Co–F bond lengths range from 1.881 to 1.964 Å and F–F bond lengths are range from 2.411 to 2.721 Å for the rutile-type structure. The Co–F bond lengths range from 1.785 to 1.987 Å and F–F bond lengths range from 2.285 to 2.677 Å for the $CaCl_2$-type structure. The Co–F bond lengths range from 1.783 to 1.876 Å and F–F bond lengths range from 2.080 to 2.709 Å for the monoclinic structure. The F is three-, three- and two- fold coordinated by Co.

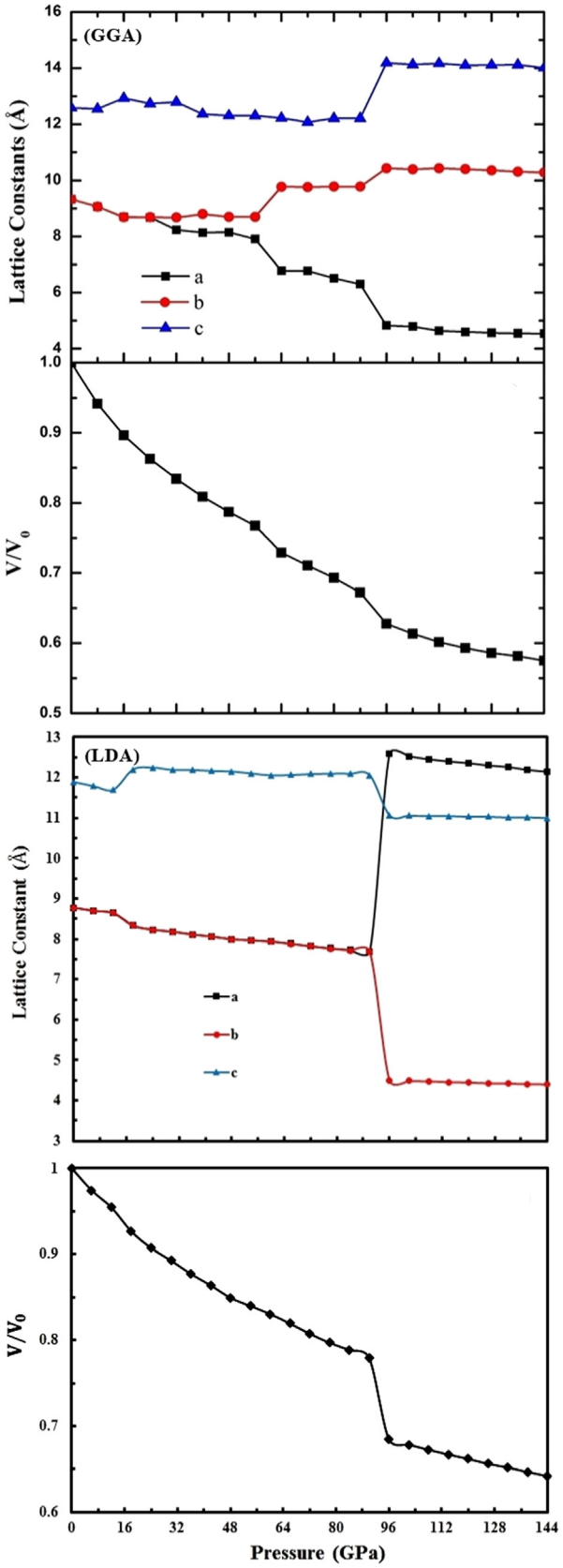

Fig. 4. (Color on-line) Volume–pressure and lattice constants–pressure relation at 64 GPa and 96 GPa with GGA method and 96 GPa with LDA method.

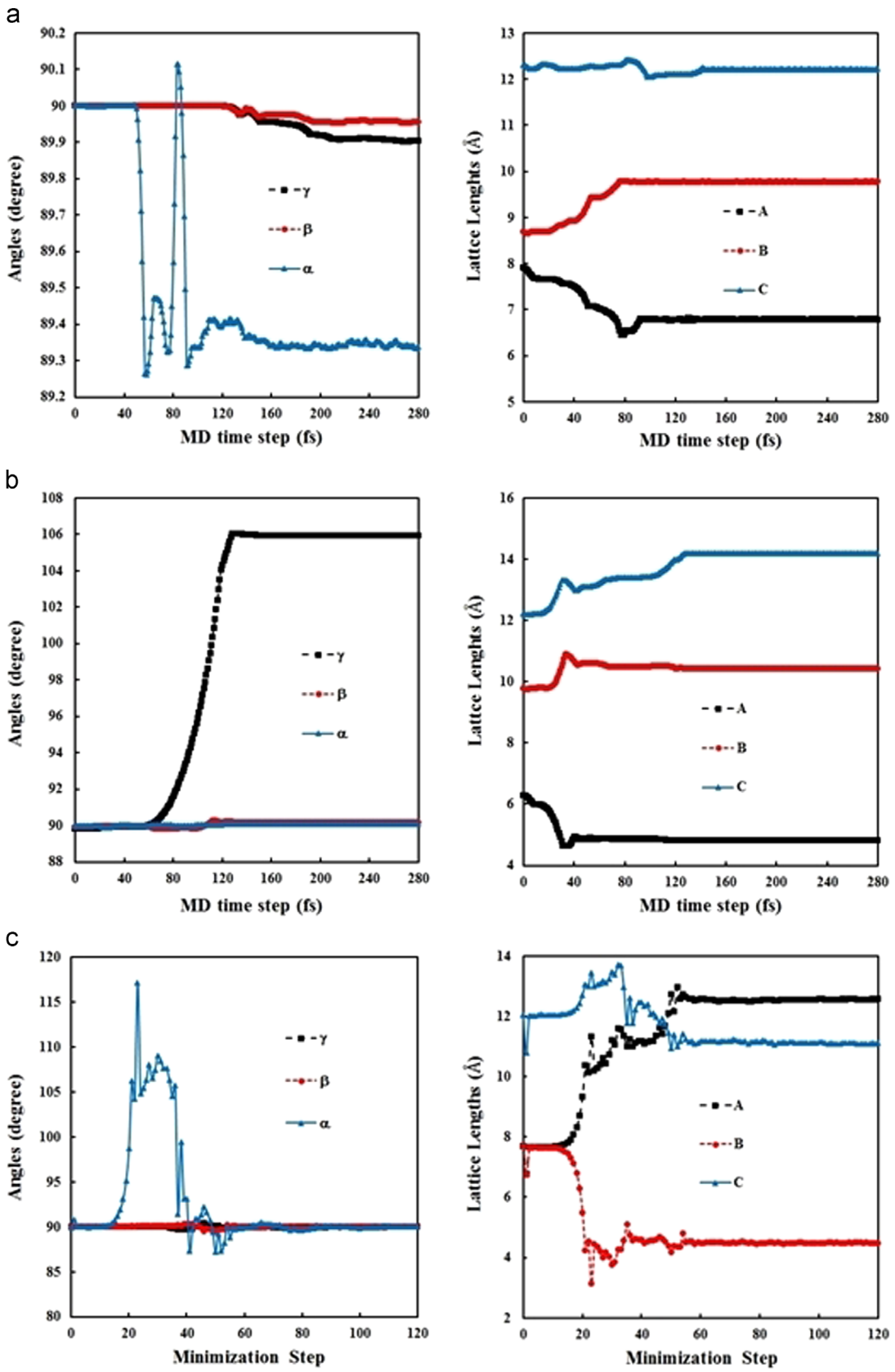

Fig. 5. (Color on-line) The simulation cell lengths and angles as a function of the MD time step at (a) 64 GPa and (b) 96 GPa with GGA method and as a function of minimization step at (c) 96 GPa with LDA method for CoF_2.

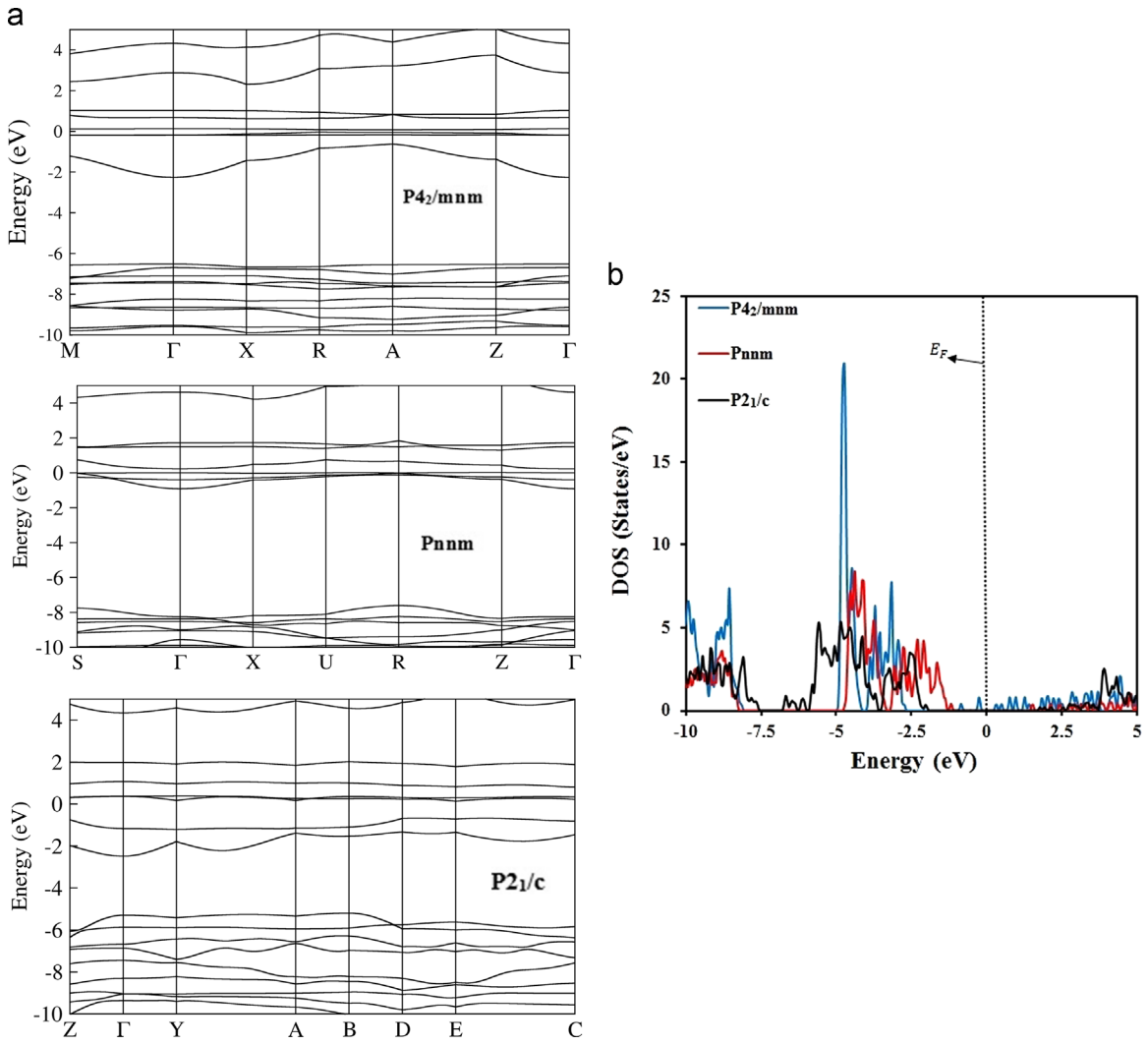

Fig. 6. (a) The calculated electronic band structures (b) density of states (DOS) of $P4_2/mnm$, Pnnm and $P2_1/c$ phases of CoF2.

By using LDA method, it was found that Co is six- and four-fold coordinated by F for the rutile-type structure and $CaCl_2$-type structure, respectively. The Co–F bond lengths range from 1.865 to 1.933 Å and F–F bond lengths range from 2.461 to 2.690 Å for the rutile-type structure. The Co–F bond lengths range from 1.777 to 1.781 Å and F–F bond lengths range from 2.126 to 2.323 Å for the $CaCl_2$-type structure. The F is three- and two- fold coordinated by Co.

In this study, tetragonal rutile-type structure of CoF_2 was firstly equilibrated at zero pressure and pressure was gradually increased up to 144 GPa with an increment of 8 GPa for GGA and 6 GPa for LDA. The structure of CoF_2 transforms from rutile-type structure with space group $P4_2/mnm$ to $CaCl_2$-type structure with space group Pnnm at 64 GPa for GGA and at 96 GPa for LDA method and $CaCl_2$-type structure to monoclinic structure with space group $P2_1/c$ at 96 GPa for the GGA method. These structures with unitcells were depicted in Fig. 3 and their lattice parameters and the atomic positions were given for GGA and LDA methods in Table 2. We plotted volume–pressure relation and lattice constants–pressure relations to determine the thermodynamic nature of the phase transitions for CoF_2 in Fig. 4. We can infer that the volume and lattice constants decrease monotonically. The phase transitions are obtained at 64 GPa and 96 GPa for GGA and 96 GPa for LDA. It is clear that the changes in volume and lattice constants are discontinuous at the transition pressure, characterizing the second-order nature. After the transition pressure, the lattice constant (a and b) increasingly diverge, suggesting an enhanced degree of orthorhombic distortion in the $CaCl_2$ phase under compression.

The simulation cell vectors A, B and C correspond along the [100], [010] and [001] directions in the beginning, respectively. The A, B and C cell lengths and γ, β and α angles are plotted as a function of MD time step so as to explain the mechanism of phase transformation. The cell lengths and angles were shown as a function of MD time step at 64 GPa and 96 GPa for the GGA method in Fig. 5a and b. The cell length and angle was shown as a function of minimization step at 96 GPa for LDA method in Fig. 5c.

We attentively analyze the structure each MD time step using the KPLOT program to investigate whether there is any intermediate phase during the phase transition or not. We didn't find any intermediary phase both GGA and LDA method.

Electronic band structures and electronic density of states (DOS) of CoF_2 for $P4_2/mnm$, Pnnm and $P2_1/c$ phases were depicted near the Fermi energy (E_F) level as a function of energy in Fig. 6a and b. Fermi level was set to be 0 eV. The symmetry points are M, Γ, X, R, A, Z and Γ for $P4_2/mnm$ phase, S, Γ, X, U, R, Z and Γ for Pnnm phase and Z, Γ, Y, A, B, D and E for $P2_1/c$ phase. As seen from electronic band structures of CoF_2, the valance band is located below the E_F level, while the conduction band is located above it. There are energy gaps (E_g) between valance and conduction band in all phases of CoF_2. This suggested that CoF_2

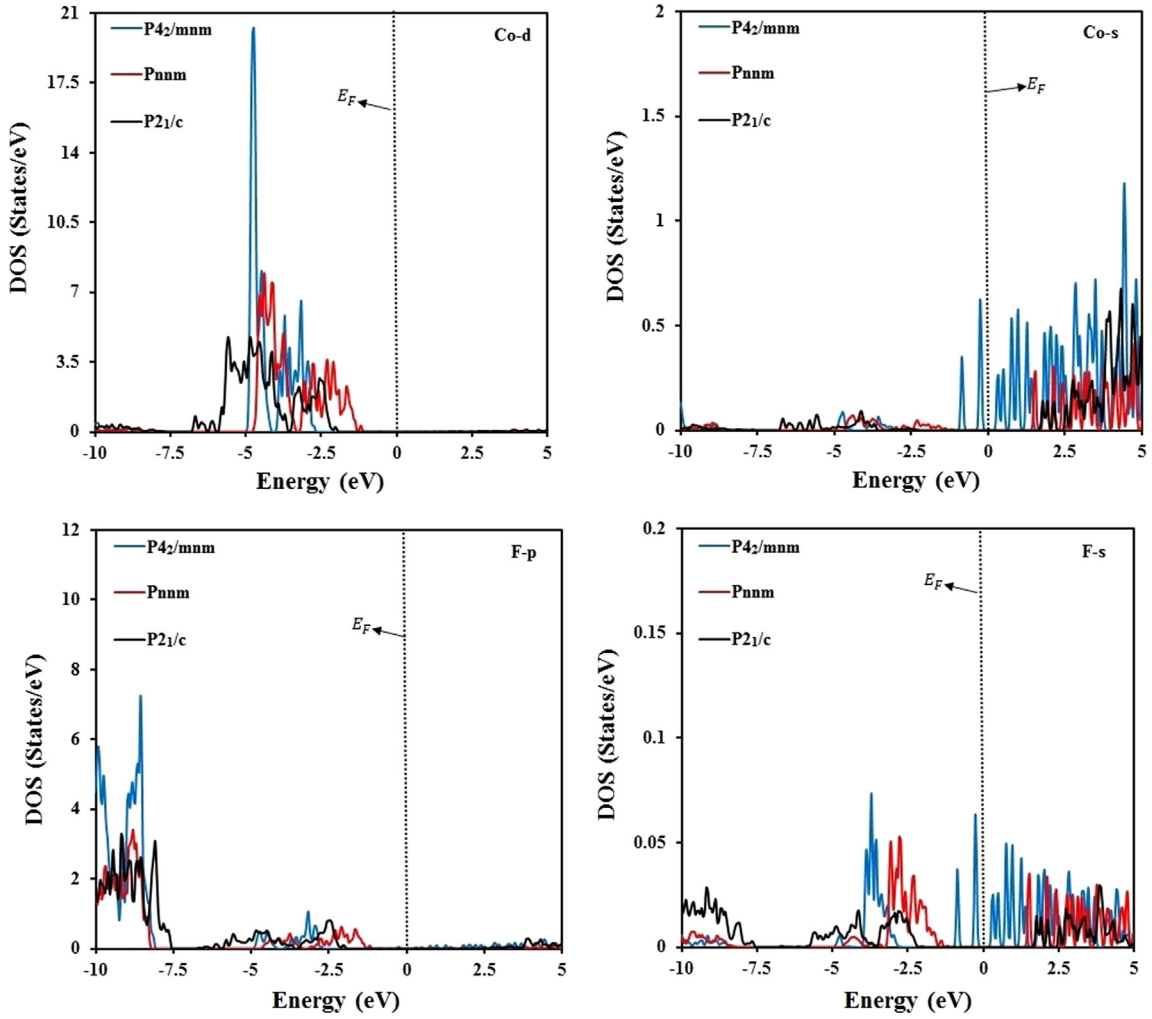

Fig. 7. The calculated partial density of states (PDOS) for CoF_2.

indicates semiconductor behavior similar with the results of Barreda et al. [25]. Energy gaps obtained from electronic band structure and DOS were approximately 0.2 eV, 2.5 eV and 3.7 eV for $P4_2/mnm$, Pnnm and $P2_1/c$ phases of CoF_2, respectively. In Fig. 7, we illustrated partial density of states (PDOS) at 0 GPA, 64 GPa and 96 GPa to understand the electronic nature of CoF_2 compound. The largest contribution came from 3d electrons of Cobalt atom in the valance band region of PDOS; and also from hybridization of "s, p" orbitals of F, and "s" orbitals of C atoms in the positive region (conduction band) of PDOS.

4. Conclusions

In summary, the crystal structure and structural phase transition of CoF_2 under high hydrostatic pressure at zero temperature have been studied using Siesta method. We found that CoF_2 is provided with three structure types for GGA and two structure types for LDA within the pressure ranging from 0 to 144 GPa. Under the influence of pressure the rutile-type structure of CoF_2 transforms irreversibly to the $CaCl_2$-type structure. The transformations were accomplished at 64 GPa for GGA and 96 GPa for LDA, and this results are in good agreement with the experimental and theoretical data. At 96 GPa, we obtained a phase transformation from $CaCl_2$-type structure to monoclinic structure for GGA method. No further transitions were observed up to 144 GPa both GGA and LDA methods. There are six atoms per unit cell in all structures both GGA and LDA. Barreda et al. [25] obtained phase transition sequence of CoF_2 as $P4_2/mnm \rightarrow Pnnm \rightarrow Pbca$ or $P\bar{a}3 \rightarrow Fm\bar{3}m \rightarrow Pnma$. First two phases and electronic properties of CoF_2 obtained from our calculations are in good agreement with the results of Barreda et al. [25].

References

[1] A.E. Austin, J. Phys. Chem. Solids 30 (1969) 1282–1285.
[2] J.D. Jorgensen, T.G. Worlton, J.C. Jamieson, Phys. Rev. B 17 (1978) 2212–2215.
[3] H. Wang, X. Liu, Y. Li, Y. Liu, Y. Ma, Solid State Commun. 151 (2011) 1475–1478.
[4] A.Y. Wu, Phys. Lett. A 60 (1977) 260–262.
[5] J.C. Jamieson, A.Y. Wu, J. Appl. Phys. 48 (1977) 4573–4575.
[6] L.C. Ming, M.H. Manghnani, T. Matsui, J.C. Jamieson, Phys. Earth Planet. Inter. 23 (1980) 276–285.
[7] L. Nagel, M. O'Keeffe, Mater. Res. Bull. 6 (1971) 1317–1320.
[8] P. Duffek, K. Schwarz, P. Blaha, Phys. Rev. B 48 (1993) 12672–12682.
[9] I. de, P.R. Moreira, R. Dovesi, C. Roetti, V.R. Saunders, R. Orlando, Phys. Rev. B 62 (2000) 7816–7823.
[10] H. Ozturk, C. Kurkcu, C. Kurkcu, J. Alloy. Comp. 597 (2014) 155–160.
[11] H. Ozturk, C. Kurkcu, C. Kurkcu, J. Alloy. Comp. 609 (2014) 185–191.
[12] S. Lopez-Moreno, A.H. Romero, J. Mejia-Lopez, A. Munoz, I.V. Roshchin, Phys. Rev B 85 (2012) 134110-1-15.
[13] W.J. Bang, C.X. Lu, Z. Hong, X.Z. Wei, Chin. Phys. B 23 (2014) 077102-1-7.
[14] S.S. Kabalkina, L.F. Vereshchagin, L.M. Lityagina, Soc. Phys. Solid State 11 (1969) 846–848.
[15] J.P. Perdew, K. Burke, M. Enzerhof, Phys. Rew. Lett 77 (1996) 3865–3868.
[16] D.M. Ceperley, B.J. Adler, Phys. Rev. Lett. 45 (1980) 566–569.
[17] P. Ordejon, E. Artacho, J.M. Soler, Phys. Rev. B 53 (R10) (1996) 441–444.
[18] N. Troullier, J.L. Martins, Phys. Rev. B 43 (1991) 1993–2006.
[19] H.J. Monkhorst, J.D. Pack, Phys. Rev. B 13 (1976) 5188–5192.

[20] R. Hundt, J.C. Schön, A. Hannemann, M. Jansen, J. Appl. Cryst. 32 (1999) 413–416.
[21] A. Hannemann, R. Hundt, J.C. Schön, M. Jansen, J. Appl. Cryst. 31 (1998) 922–928.
[22] F. Birch, Phys. Rev. 71 (1947) 809–824.
[23] F.D. Murnaghan, Proc. Natl. Acad. Sci. USA 30 (1944) 244–247.
[24] M.M.R. Costa, J.A. Paixao, M.J.M. de Almeida, L.C.R. Andrade, Acta Cryst. B49 (1993) 591–599.
[25] J.A. Barreda-Argüeso, S. Lopez-Moreno, M.N. Sanz-Ortiz, F. Aguado, R. Valiente, J. Gonzalez, F. Rodriguez, A.H. Romero, A. Munoz, L. Nataf, F. Baudelet, Phys. Rev. B 88 (2013) 214108-1-15.